Pulsed Laser Ablation of Metal Plate in Supercritical Carbon Dioxide

Motonobu Goto[1]*, Siti Machmudah[1], Wahyudiono[2], Yutaka Kuwahara[2], Mitsuru Sasaki[2]

[1] Bioelectrics Research Center, Kumamoto University, Kumamoto 860-8555 Japan

[2] Graduate School of Science and Technology, Kumamoto University, Kumamoto 860-8555, Japan

*E-mail: mgoto@kumamoto-u.ac.jp; Fax: +81-96-342-3665

Nanosecond pulsed laser ablation (PLA) of copper and gold plate with an excitation wavelength of 532 nm was carried out in supercritical CO_2. Surface morphology of the plates after irradiation and the crater depth after PLA were observed by laser scanning microscopy, while extinction spectra of nanoparticles collected in the glass slide was measured by UV-Vis spectrophotometer. Copper and gold plates were ablated at various supercritical CO_2 densities and irradiation times at constant temperature of 40^{o}C. Both surface morphology of irradiated plate and crater depth formation were significantly affected by the changes in supercritical CO_2 density, the surrounding environment and irradiation time. As expected the increasing supercritical CO_2 density resulted deeper ablation crater, however the deepest crater for gold plate was obtained at density of 0.63 g/cm^3 or pressure of 10 MPa. Gold nanoparticles generated by PLA in $SCCO_2$ have been confirmed at the spectra band near 530.

INTRODUCTION

Having a zero surface tension, the supercritical fluid allows complete penetration into metal cavity. Furthermore, the lower viscosity of supercritical fluid in comparison with the liquids can reduce the solvent-cage effects and therefore increase the initiator efficiency. Since the solvent power of supercritical fluid is directly related to its density, a large variation in solubility can be achieved by simply changing the pressure and temperature of the system. Moreover, by simple pressure reduction, phase change is observed, and the supercritical fluid is transformed to a gas and exits the system without leaving any residues. Supercritical CO_2 ($SCCO_2$) has been widely applied in a variety of processes including extraction, separation, and material processing. Recently, it has been found that supercritical fluids such as $SCCO_2$ and supercritical water produce interesting reaction fields for nanotechnology [1, 2] and plasma technology [3].

Pulsed laser ablation (PLA) has been widely employed in industrial and biological applications and in other fields. The environmental conditions in which PLA is conducted are important parameters that affect both the solid particle cloud (plume) and the deposition (debris) produced by the plume. In most studies, particles are generated either in a vacuum or in ambient conditions. Some studies, however, use a different ambient medium such as a gas, a surfactant solution [4, 5], organic solvent [6], liquid N_2 [7], and $SCCO_2$ [8-10]. Saitow et al. have reported that silicon nanoclusters and gold nanonecklaces could be generated by performing PLA in $SCCO_2$ [8, 9]. However, they did not discuss the synthesis behavior in much detail. Moreover, only those two investigations of PLA in $SCCO_2$ have been reported. In this work, PLA of copper and gold substrate in $SCCO_2$ was conducted to generate

synthesized metal nanoparticles. The effect of ablation environment, CO_2 density and irradiation time on the irradiated plate was investigated. The surface morphology of irradiated plate and generated nanoparticles were observed.

EXPERIMENTAL METHODS

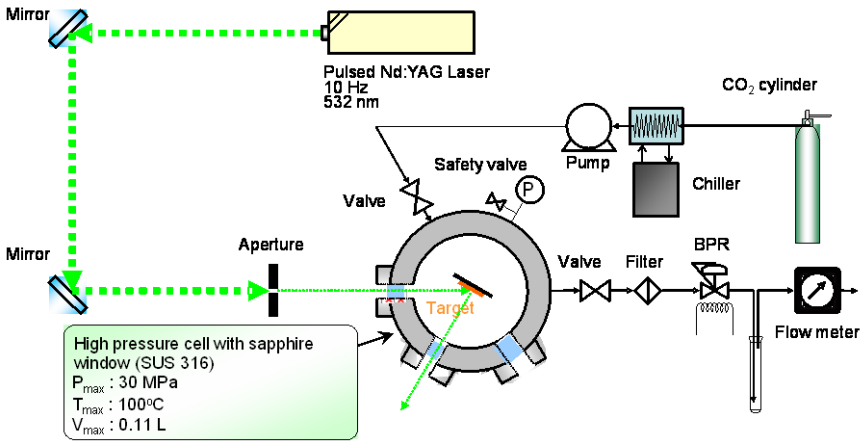

Figure 1 Experimental apparatus of pulse laser ablation (PLA) with a high pressure cell

PLA was carried out in a high-pressure cell with three sapphire windows. **Figure 1** shows the schematic diagram of the experimental apparatus. The second harmonic of a Q-switched pulsed Nd:YAG laser (Spectra-Physics Quanta-Ray INDI-40-10, wavelength: 532 nm, pulse energy: maximum 200 mJ/(cm^2.pulse), pulse duration: 8 ns, repetition frequency: 10 Hz) was used. Target was fixed in a high-pressure cell (AKICO). Incident angle of the laser beam was 30^o and the laser was located 1 m from the target. A gold plate (Nilaco, purity: 99.99%, thickness: 0.03 mm) was used as the target. Liquid CO_2 was pressurized and pumped into the cell using a high pressure pump. A glass slide was placed in parallel with the target to collect metal nanoparticles. The cell temperature was controlled by a temperature controller. The cell temperature was maintained at 40^oC, as measured by a thermocouple. The pressure of the system was varied from 0.1 to 25 MPa. After the temperature and pressure were stable, PLA was carried out for 3000 and 5000 s. The laser beam was collimated by a 1-mm-diameter of aperture without any focusing lens. PLA was also conducted in air at ambient condition. The surface morphology of the target after irradiation and the crater depth after PLA were observed by laser scanning microscopy. Absorption spectrum of metal nanoparticles collected in the glass slide was also evaluated by UV-Vis spectrophotometer.

RESULTS AND DISCUSSION

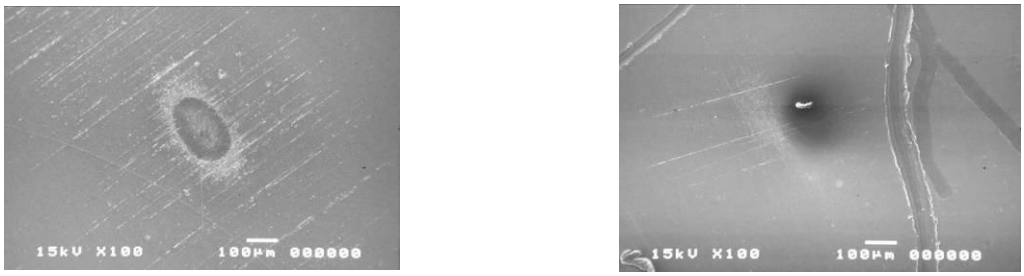

Figure 2 SEM images of Cu plate after ablation by Nd:YAG laser (a) in $SCCO_2$ (25 MPa, 180 sec, fluence before a high-pressure cell; 224 mJ/cm^2/pulse), and (b) in air (0.1 MPa, 180 sec, fluence before a high-pressure cell; 228 mJ/cm^2/pulse)

Figure 2 shows SEM micrographs of the Cu plate after PLA in $SCCO_2$. An elliptical crater is clearly observed in the center of the irradiated region after PLA in $SCCO_2$, and slight rough surface is appeared around the crater. In contrast, there were only slight indications of ablation on the surface of Cu plate after PLA in air and in hexane.

Figure 3 shows laser micrographs after PLA of Cu plates in $SCCO_2$ and in air; the ablation depth can be seen in these micrographs. A crater is clearly observed on the Cu plate after ablation in $SCCO_2$.

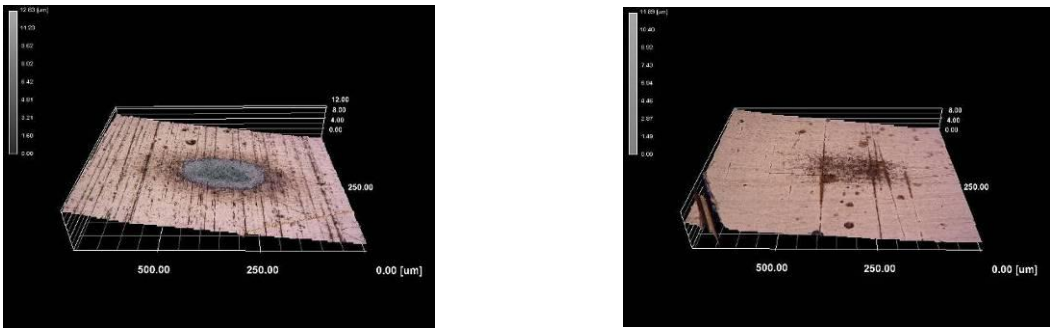

Figure 3 Laser microscopy images of Cu plate ablated by Nd:YAG laser (a) in $SCCO_2$ (25 MPa 180 sec, fluence before a high-pressure cell l; 224 mJ/cm^2/pulse), (b) in air (180 sec, fluence before a high-pressure cell; 228 mJ/cm^2/pulse)

Figure 4 shows the dependence of ablation depth on irradiation time after PLA in $SCCO_2$ and in air. The ablation depth in $SCCO_2$ increased with an increase in irradiation time for pressures of 10 and 25 MPa. The maximum ablation depth was achieved in $SCCO_2$ at a pressure of 25 MPa. For ablation in $SCCO_2$, the ablation efficiency at 25 MPa is twice higher than that at 10 MPa. An ablation crater with a depth of 6.9 μm was observed at temperature of 40ºC, pressure of 25 MPa, and irradiation time of 500 s. In contrast, the correct depth of craters after PLA in air was too slight to estimate the irradiation time dependence of ablation depth by the laser microscope observation. It is known that a copper target may have thin oxide layer on the surface [11]. In this study, all targets may generate several nanometers of thin oxide layer for polishing with alumina compounds as the pretreatment. However, it can be seen that the presence of nanometer-sized oxide layer has no influence on the micrometer-sized depth of the crater ablated by thousands times of laser irradiation.

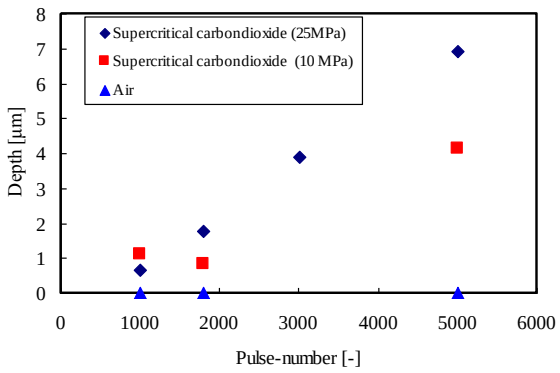

Figure 4 Dependence of irradiation time for ablation of Cu plate in $SCCO_2$ and air.

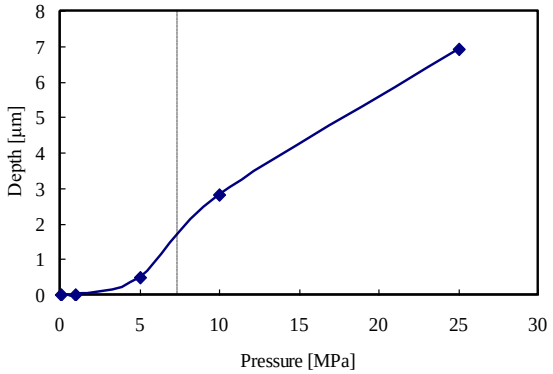

Figure 5 The pressure dependence of the ablation depth of Cu plate with 500 seconds of irradiation time.

The effect of pressure on ablation depth in $SCCO_2$ condition at irradiation time of 500 s is shows in **Figure 5**. As expected, the increasing pressure caused the increasing ablation depth due to the change of $SCCO_2$ properties.

Surface morphology of gold plate after ablation at 40^{o}C and various pressures for 3000 s is shown in **Figure 6**. A circle crater was clearly observed in the irradiated gold plate at all conditions. The crater was more clearly generated as increasing pressure. In addition, the surface around irradiation region was slightly rough due to the solid particle cloud (plume) deposited. However, the hole was only generated at 10 MPa of PLA in $SCCO_2$. The increasing pressure of CO_2 caused increasing density of CO_2, on the other hand constant volume heat capacity of CO_2 decreases from 10 to 20 MPa. It caused stronger PLA in $SCCO_2$ at 10 MPa, and as the result PLA could generate the hole in the gold plate.

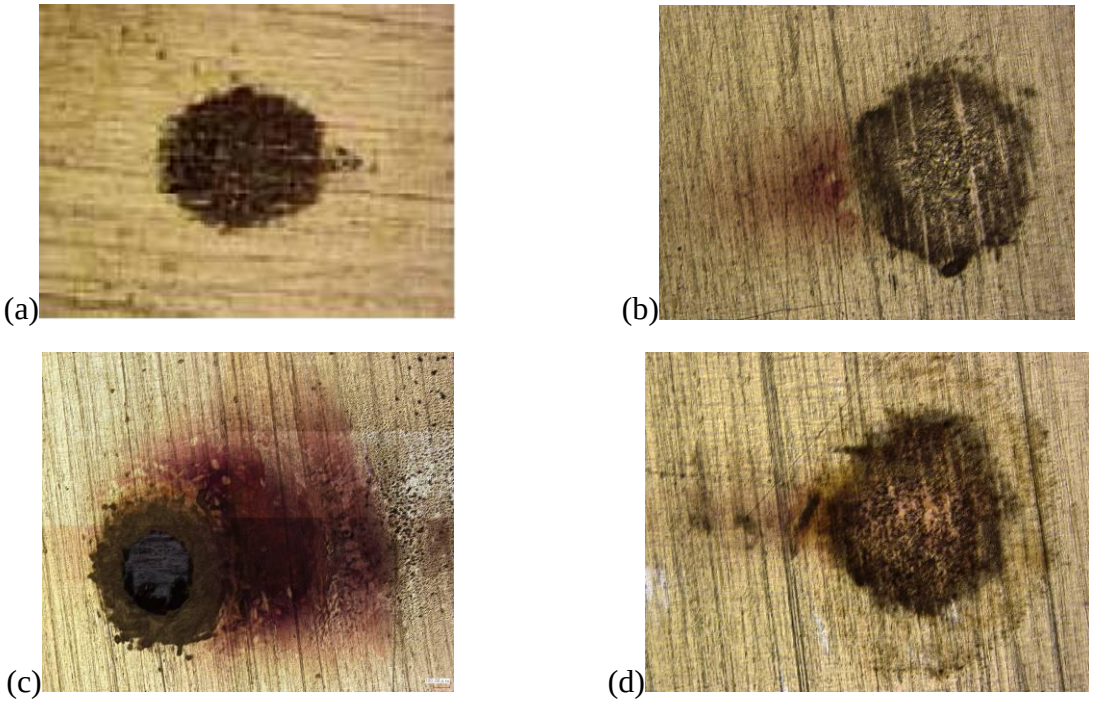

Figure 6 Laser scanning microscopy image of Au plate after ablation at 40^{o}C for 3000s by Nd:YAG laser. (a) in air at ambient pressure; (b) in liquid CO_2 at 6.5 MPa; (c) in $SCCO_2$ at 10 MPa; (d) in $SCCO_2$ at 20 MPa

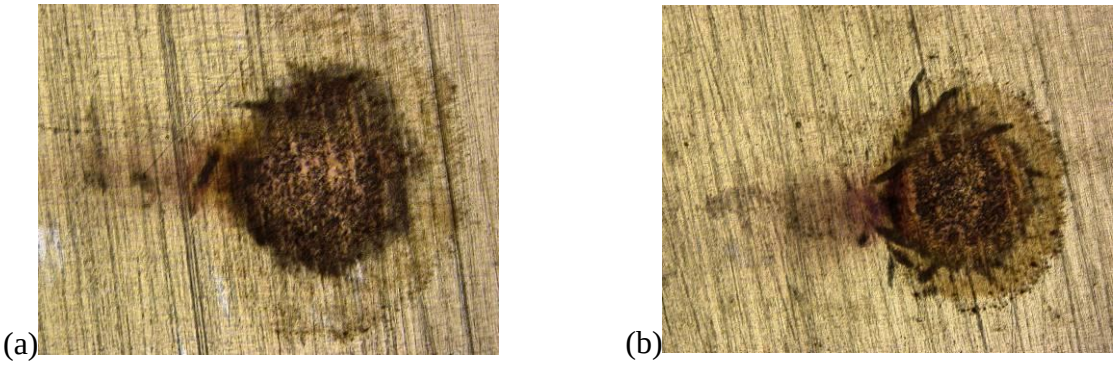

Figure 7 Laser scanning microscopy image of Au plate after ablation in $SCCO_2$ at 40^{o}C and 20 MPa by Nd:YAG laser. (a) 3000 s; (b) 5000 s

Surface morphology of ablated gold plate at various irradiation times is shown in **Figure 7**. The ablation was studied at 40^{o}C and 20 MPa. As increasing irradiation time, plume deposited in the surrounding crater was clearly observed. It can be explained that plume generated by PLA becomes larger with increasing irradiation time.

To determine the depth of crater generated by PLA in $SCCO_2$, 3D laser scanning microscopy image was analyzed, as shown in **Figure 8**. **Figure 9** shows the crater depth generated by PLA at various pressures. As expected, the increasing pressure causes increasing the crater depth due to CO_2 properties change in the system. However, the deepest crater was observed at 10 MPa due to higher constant volume heat capacity of CO_2 at the condition. The crater depth at 10 MPa was thicker than initial gold plate thickness because the plume deposited around the hole was generated.

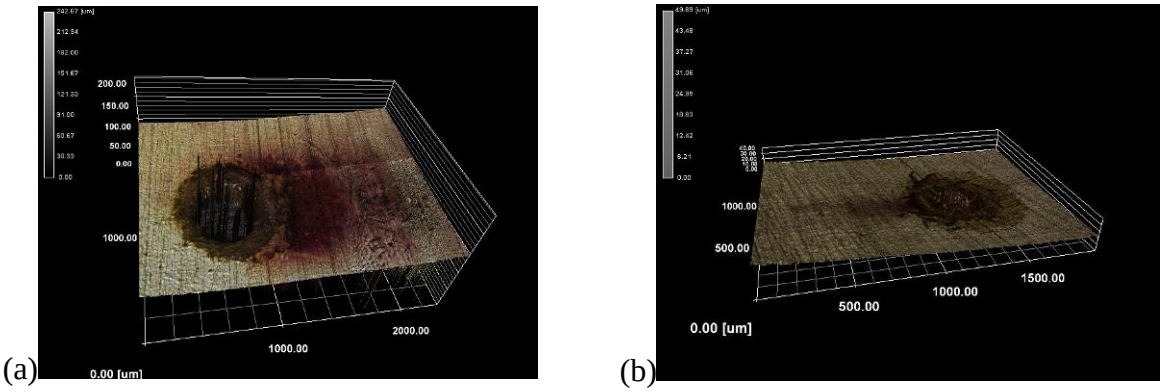

Figure 8 3D laser scanning microscopy image of Au plate after ablation in $SCCO_2$ at 40^{o}C. (a) 10 MPa; (b) 20 MPa

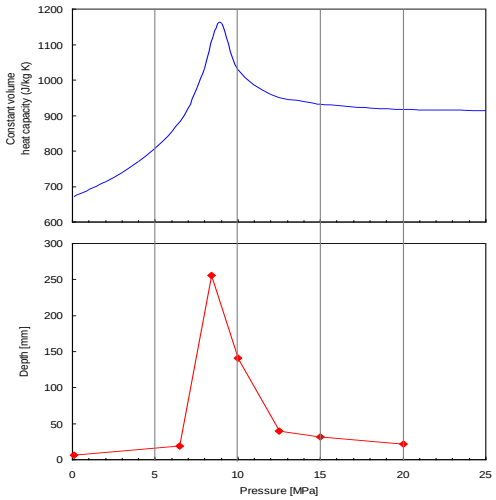

Figure 9 Depth of crater generated by PLA at various pressures

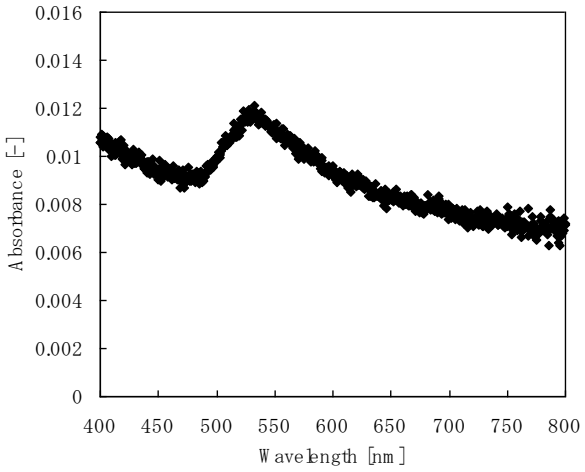

Figure 10 Extinction spectra of gold nanoparticles deposited in glass slide at 40^{o}C and 20 MPa for 3000 s

Extinction spectra of gold nanoparticles deposited in glass slide was also measured for confirmation of generated gold nanoparticles. **Figure 10** shows the spectra of generated gold

nanoparticles in glass slide, measured after CO_2 depressurizing. The spectra contain bands near 530 and 650. The peak near 530 nm has been known to correspond to the plasmon band of gold nanospheres with diameters <50 nm [9]. As reported by Saitow et al. [9], the plasmon band near 530 nm, which is due to nanospheres smaller than 50 nm in diameter, is independent on density, whereas the bands near 650 nm varies with density.

CONCLUSION

Laser ablation of copper and gold plates has been conducted in $SCCO_2$ at various densities and irradiation times. The surface morphology of the metal plate after irradiation and the crater depth after PLA were observed by laser scanning microscopy. For gold plate ablation, extinction spectra of gold nanoparticles collected in the glass slide was measured by UV-Vis spectrophotometer. Surface morphology of metal plate after ablation was dependent on CO_2 density and pressure. The depth of crater generated by PLA increased as increasing density and pressure. However, the deepest crater for gold plate was obtained at 10 MPa of ablation. Gold nanoparticles generated by PLA in $SCCO_2$ have been confirmed at the spectra band near 530.

ACKNOWLEDGEMENT

This work was supported by Kumamoto University Global COE Program "Global Initiative Center for Pulsed Power Engineering" and Japan Society for the Promotion of Science (JSPS).

REFERENCES:

[1] Kameo, A., Yoshimura, T., Esumi, K., *Colloids Surf. A*, 215, **2003**, 181

[2] Adschiri, T., *Chem. Lett.*, 36, **2007**, 1188

[3] Kiyan, T., Sasaki, M., Ihara, T., Namihira, T., *Plasma Process. Polym.*, 6, **2009**, 778

[4] Masanori Hara, Motonobu Goto, Hidenori Akiyama

[5] He, C., Sasaki, T., Shimizu, Y., Koshizaki, N., *Appl. Surf. Sci.*, 254, **2008**, 2196

[6] Liang, C., Shimizu, Y., Masuda, M., Sasaki, T., Koshizaki, N., *Chem. Mater.*, 16, **2004**, 963

[7] Amendola, V., Rizzi, G. A., Polizzi, S., Meneghetti, M., *J. Phys. Chem.*, 109, **2005**, 23125

[8] Takada, N., Ushida, H., Sasaki, K., *J. Phys.: Conf. Ser.*, 59, **2007**, 40

[9] Saitow, K., *J. Phys. Chem. B*, 109, **2005**, 3731

[10] Saitow, K., Yamamura, T., Minami, T., *J. Phys. Chem. C*, 112, **2008**, 18340

[11] Kuwahara, Y., Saito, T., Haba, M., Iwanaga, T., Sasaki, M., Goto, M., *Jpn. J. Appl. Phys.*, 48, **2009**, 040207

[12] Yonezawa, Y., Minamikawa, T., Morimoto, A., Shimizu, T., *Jpn. J. Appl. Phys.*, 37, **1998**, 4505